Pure Appl. Chem., Vol. 82, No. 8, pp. 1701–1717, 2010.
doi:10.1351/PAC-CON-09-09-30

On the formation of uranium(V) species in alkali chloride melts*

Vladimir A. Volkovich[1,‡], Denis E. Aleksandrov[1], Trevor R. Griffiths[2], Boris D. Vasin[1], Timur K. Khabibullin[1], and Dmitri S. Maltsev[1]

[1]Department of Rare Metals and Nanomaterials, Ural State Technical University—UPI, Ekaterinburg, 620002, Russia; [2]Redston Trevor Consulting Ltd., Leeds, LS17 8RF, UK

Abstract: Uranyl(V) species are normally unstable in solutions but are here shown to be stable in high-temperature chloride melts. Reactions leading to the formation of $UO_2Cl_4^{3-}$ ions were studied, including thermal decomposition and chemical reduction of uranyl(VI) chloro-species in various alkali chloride melts (LiCl, 3LiCl–2KCl, NaCl–KCl, and NaCl–2CsCl) at 550–850 °C. Decomposition of $UO_2Cl_4^{2-}$ species under reduced pressure, with inert gas bubbling through the melt or using zirconium getter in the atmosphere results in the formation of $UO_2Cl_4^{3-}$ and UO_2. Elemental tellurium, palladium, silver, molybdenum, niobium, zirconium, and hydrogen, as well as niobium and zirconium ions were tested as the reducing agents. The outcome of the reaction depends on the reductant used and its electrochemical properties: uranyl(VI) species can be reduced to uranyl(V) and uranium(IV) ions, and to uranium dioxide.

Keywords: molten salts; reduction; spectroscopy; uranium; uranyl.

INTRODUCTION

Uranium(V) is the least studied of all oxidation states of uranium in solutions. Aqueous solutions of UO_2^+ are prone to disproportionation, and the 5+ oxidation state of uranium has a very narrow range of existence in this medium [1], with the carbonate complex $UO_2(CO_3)_3^{5-}$ being the most stable species [2]. Several U(V) complexes have been characterized in organic solvents [3] and uranium(V) species are stable in ionic solvents. The electronic absorption spectra of uranyl(V) chloro-complexes in chloride melts were reported nearly half a century ago [4,5]. Electrochemical and thermodynamic [6], and structural [7] studies of UO_2^+ in high-temperature chloride melts have subsequently been performed, and the behavior of uranium(V) in low-temperature melts has also been considered [8].

Pentavalent uranium in high-temperature melts exists in the form of complexes of oxo-cations. Investigations concerning uranium(V) in molten salts have mostly been limited to studying the behavior and properties of the compounds formed rather than the reactions leading to their formation, with the exception perhaps of thermal decomposition and electrochemical reduction of U(VI). At elevated temperatures, uranyl(VI) chloride decomposes losing Cl_2. Such reaction also takes place in chloride melts but there is no agreed opinion concerning products of such decomposition. Wilks [9] reported that during the decomposition of uranyl(VI) chloride dissolved in a chloride melt Cl_2 is evolved and U_3O_8

---

*Paper based on a presentation on the "Synthesis and Mechanism" theme at the 42nd IUPAC Congress, 2–7 August 2009, Glasgow, UK. Other Congress presentations are published in this issue, pp. 1569–1717.

‡Corresponding author

is precipitated. According to Wenz and Adams [4], uranyl(V) ions are formed in the melt below 750 °C: at higher temperatures UO_2 is precipitated and a small amount of U(IV) ions is formed in the melt. Adams [5] and Stromatt [10] attributed the formation of UO_2^+ ions in the melt to the reaction between UO_2^{2+} and uranium dioxide. Somewhat later, Smirnov et al. [11] reported that upon removing Cl_2 from the atmosphere above a uranyl(VI)-containing melt, U_3O_8 and uranium tetrachloride are formed.

Electrochemical reduction of $UO_2Cl_4^{2-}$ to UO_2 proceeds stepwise via U(V) as intermediate. Nagai et al. [12] employed high-temperature spectroscopy to study the potentiostatic reduction of $UO_2Cl_4^{2-}$ to $UO_2Cl_4^{3-}$ in a NaCl–2CsCl melt at 650 °C.

U(V) species in melts can be produced by reducing U(VI) or oxidizing a lower oxidation state of uranium. Previously [13], we investigated the reaction of uranium dioxide with hydrogen chloride in a series of alkali chloride melts and found that under certain conditions (depending on temperature and cationic melt composition) the reactions led to the oxidation of UO_2 to form soluble uranium(V) species, $UO_2Cl_4^{3-}$. The present work was aimed toward studying the chemical reduction and decomposition of uranyl(VI) species in molten alkali metal chlorides.

EXPERIMENTAL

Experiments were performed in melts based on LiCl, NaCl–KCl equimolar mixture, and 3LiCl–2KCl and NaCl–2CsCl eutectics at temperatures between 550 and 850 °C. Starting alkali metal chlorides (of analytical purity) were dried at 300 °C under vacuum for several hours, after which the temperature was raised to ca. 100 ° above the melting point and the molten salts were kept under vacuum for 4–5 h before cooling. These dried salts were subsequently melted, and dry hydrogen chloride was bubbled through them for 5 h to convert any oxide impurities present into chlorides. Salt mixtures having the required composition were prepared by mixing together the individual alkali chlorides and then fusing them under vacuum. Prior to experimentation, all salt mixtures were subjected to zone refining 5–8 times under vacuum.

Electronic absorption spectra were recorded using a custom-built set-up based on a double-channel fiber optic spectrometer Avantes AvaSpec-2048-2 and a single-channel AvaSpec-NIR256-1.7 that together allowed measurement of spectra between 210 and 1350 nm. Melts (normally 6–10 ml) were held in 1-cm path-length optical silica cells attached to silica tubes with side-arms and stoppers containing the necessary electrodes and attachments. Electrochemical measurements were performed employing an Autolab PGSTAT302N potentiostat/galvanostat. All electrode potentials were measured vs. Ag/AgCl (1 mol % in NaCl–2CsCl) reference electrode. The standard silver potential (relative to Cl_2/Cl^- reference electrode) in NaCl–2CsCl melt can be calculated from the following equation [14]:

$$E^*\mathrm{Ag(I)/Ag} = (-1.223 + 3.26\ 10^{-4}\ T) \pm 0.008\ \mathrm{V} \qquad (1)$$

The starting uranyl(VI)-containing melts were prepared by reacting UO_2 or U_3O_8 with Cl_2 in the chosen alkali chloride melts. These concentrated melts (containing around 10 wt % uranium) were subsequently used for preparing working melts. For spectroscopy measurements, the initial melts were prepared by dissolving a concentrated sample of quenched melt containing UO_2Cl_2 in a chosen salt-solvent so that the initial uranium concentration was about 1 wt %.

Elemental molybdenum, silver, palladium, tellurium, zirconium, and niobium (commercially available above 99 % purity) were used as reducing agents. Molybdenum wire (2 mm diameter) was lowered into the uranyl(VI)-containing melt, and the progress of the reaction was followed by both recording the electronic absorption spectra and the electrode potentials using molybdenum and glassy carbon electrodes. A similar procedure was used with silver. Palladium foil attached to a silica capillary was dipped into the melt, and metallic niobium, zirconium, and tellurium were dropped into the melt as pieces of suitable size.

When studying the reaction of uranyl(VI)-containing melts with niobium and zirconium ions, the starting melts were prepared by dissolving zirconium(IV) chloride or niobium(V) chloride in a chosen alkali chloride mixture or by anodically dissolving metallic niobium (to obtain melts containing Nb(III) and (IV) ions). A sample of uranyl(VI)-containing quenched melt was then dropped into niobium- or zirconium-containing melt.

After each experiment, a sample of melt was withdrawn into a silica capillary using a syringe and rapidly quenched. Quenched melts were analyzed for uranium and other metals (if added) content, and an average uranium oxidation state was also estimated from the results of a redox titration [15]. For this, a sample of the melt that was rapidly quenched was dissolved in a known excess of ammonium vanadate solution (in 5 M sulfuric acid) that oxidized all uranium to U(VI). The excess of vanadium(V) was then titrated with a solution of iron(II)-ammonium sulfate (also in 5 M H_2SO_4) and the average oxidation state of uranium in the sample calculated using the following expression:

$$n(\mathrm{U}) = 6 - [(C_\mathrm{V}\cdot V_\mathrm{V} - C_\mathrm{Fe}\cdot V_\mathrm{Fe})\cdot M_\mathrm{U}]/[m\cdot C_\mathrm{U}] \quad (2)$$

where n(U) is the average uranium oxidation state; C_V and C_Fe are the molar concentrations of ammonium vanadate and iron(II)-ammnium sulfate solutions, respectively; V_V and V_Fe are the volumes of ammonium vanadate and iron(II)-ammnium sulfate solutions, respectively; M_U is the molar weight of uranium; m is the weight of the melt sample; and C_U is the weight fraction of uranium in the melt. The effect of additional metals on the results of redox analysis was corrected using the known content and oxidation state determined from spectroscopy measurements (e.g., molybdenum was assumed to be present in the as $MoCl_6^{3-}$). IR spectra of quenched melt samples were measured on a Vertex 70 spectrometer (Bruker).

RESULTS AND DISCUSSION

Decomposition of uranyl(VI) chloride

Based on literature reports [4,5,9–11], the following reactions, describing the thermal decomposition of uranyl(VI) chloride dissolved in a chloride melt, can be proposed:

$$UO_2Cl_4^{2-} \rightarrow UO_2 + Cl_2 + 2Cl^- \quad (3)$$

$$UO_2Cl_4^{2-} + Cl^- \rightarrow UO_2Cl_4^{3-} + \tfrac{1}{2}Cl_2 \quad (4)$$

$$4UO_2Cl_4^{2-} \rightarrow U_3O_8 + UCl_6^{2-} + 6Cl^- + 2Cl_2 \quad (5)$$

The main discrepancy in the literature data [4,5,9–11] concerns the possibility of the formation of uranium(IV) ions as a product of decomposition of uranyl(VI) chloride. Absorption spectroscopy offers a convenient way for identifying uranium ions in different oxidation states.

The thermal decomposition of $UO_2Cl_4^{2-}$ species under vacuum ($5\cdot10^{-3}$ mm Hg) was followed here by in situ spectroscopy measurements at 550–850 °C in 3LiCl–2KCl, NaCl–KCl, and NaCl–2CsCl melts. During prolonged evacuation at higher temperatures, some solvent salt was sublimed, particularly with the cesium-containing melt, e.g., at 850 °C after 40 min the volume of the melt was reduced almost by half with sublimed salt condensed in the upper cold part of the cell.

In the course of the experiments, the yellow color of the initial uranyl(VI)-containing melts changed to brown and the absorbance in the visible region increased. The behavior in all the melts studied was similar. All spectra contained a broad band at around 770 nm, typical of $UO_2Cl_4^{3-}$ absorption in chloride melts [4,5] and arising from a $\varphi_{5u} \rightarrow 3\pi_{1u}$ transition [16]. A second band at around 620 nm ($\varphi_{5u} \rightarrow 3\pi_{3u}$ transition [16]) was hidden under a low-energy edge of a charge-transfer band. An example of the spectra recorded in NaCl–KCl melt is given in Fig. 1, and the results of the experiments conducted are summarized in Table 1. No absorption bands that could be attributed to U(IV) chloro-ions were observed.

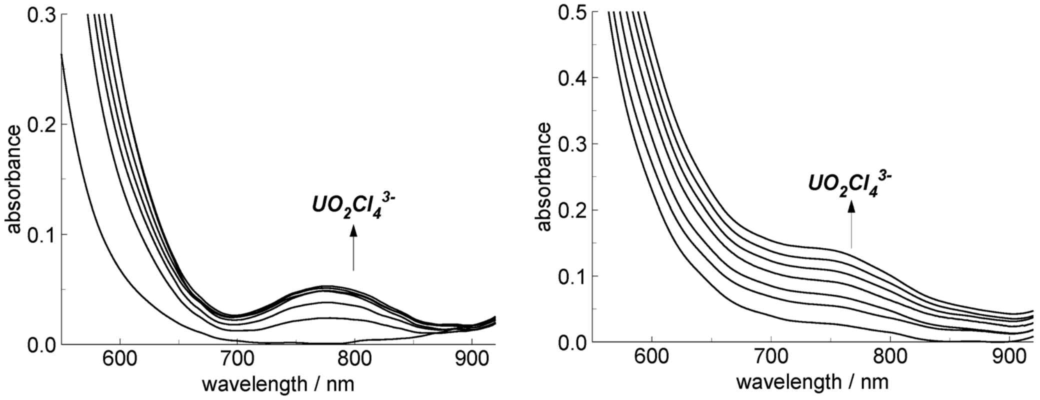

Fig. 1 Changes in the spectra of NaCl–KCl melt containing $UO_2Cl_4^{2-}$ species and held under vacuum at 750 °C for 240 min (left) and at 850 °C for 206 min (right). Initial uranium concentration was around 0.9 wt %. Arrows indicate spectral changes with time.

Table 1 Decomposition of uranyl(VI) chloro-species in alkali chloride melts under vacuum.

Melt	T, °C	Time held under vacuum, min	U conc., wt % initial	U conc., wt % final	Final U oxidation state
3LiCl–2KCl	550	340	0.76	0.53	5.7
	750	265	0.90	0.67	5.7
NaCl–KCl	750	240	0.96	0.78	5.8
	850	206	0.86	0.79	5.7
NaCl–2CsCl	650	92	0.29	0.26	5.7
	650	150	1.15	1.22	5.9
	750	173	1.13	1.59[a]	5.9
	850	40	1.18	2.00[a]	5.3

[a] Volume of the melt was significantly reduced due to solvent-salt sublimation.

Increasing the temperature resulted in a somewhat more rapid rate of decomposition. IR spectra of quenched melt samples after thermal decomposition contained bands due to U–O stretching in uranyl(VI) and uranyl(V) groups, Fig. 2. It can be noted that some uranyl(V) disproportionation (to uranyl(VI) and UO_2) could occur upon quenching the liquid melt, especially from higher temperatures. The results in Fig. 2, however, show that the intensity of uranyl(V) band was growing with temperature, thus showing that uranium(V) content in the liquid melt was higher at elevated temperature.

Cationic melt composition had a more pronounced effect: at 750 °C the rate of decomposition was highest in the 3LiCl–2KCl eutectic and lowest in the NaCl–2CsCl eutectic, with the NaCl–KCl equimolar mixture occupying an intermediate position. Smaller alkali metal cations have a greater destabilizing effect on $UO_2Cl_4^{2-}$ ions, and the stability of uranyl(VI) complex in chloride melts therefore decreases upon changing the melt cation from Cs^+ to Li^+.

Another method of Cl_2 removal from the experimental cell was sparging the melt with argon. Bubbling pure Ar gas through NaCl–2CsCl–UO_2Cl_2 melt resulted in sweeping the Cl_2 formed from the atmosphere above the melt as well as assisting conversion of $UO_2Cl_4^{2-}$ into $UO_2Cl_4^{3-}$. The presence of O_2/air impurities in argon, however, leads to the formation of insoluble alkali metal uranates.

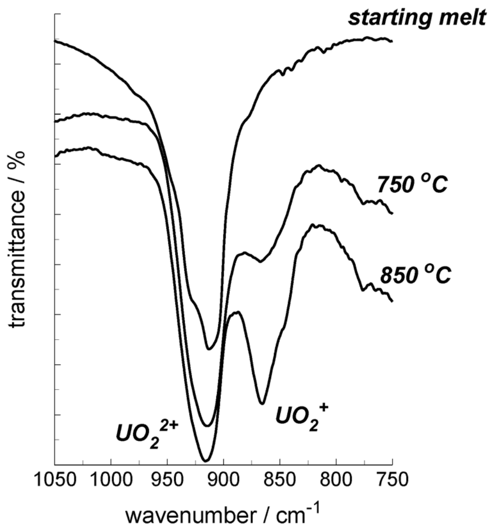

Fig. 2 IR spectra of quenched NaCl–KCl-based melts containing UO_2Cl_2 before and after heating under vacuum.

Thermodynamic calculations show that the equilibrium Cl_2 pressure above alkali chloride melts containing $UO_2Cl_4^{2-}$, $UO_2Cl_4^{3-}$, and UO_2 is below 10^{-5} mm Hg (such low pressure could not be achieved with the vacuum system employed in the present study). To lower chlorine pressure in the atmosphere in the experimental cell, a zirconium metal getter was positioned 15 mm above the melt surface. At working temperatures, zirconium easily reacts with chlorine and the equilibrium pressure of Cl_2 in the presence of Zr metal is below 10^{-10} mm Hg. The experiments were conducted between 550 and 750 °C in several melts, and the results are summarized in Table 2. During the reaction, uranyl(V) ions, $UO_2Cl_4^{3-}$, and some uranium dioxide were formed in the melt and a black compound (most likely a low-oxidation-state zirconium chloride) was deposited on the surface of zirconium turnings acting as a getter. An example of the spectra recorded is presented in Fig. 3. Final melts contained a mixture of uranyl(V) and (VI) ions; no soluble U(IV) chloro-species were present. Concentration changes of uranyl(V) species were monitored using the absorbance around 780 nm and preliminary determined U(V) molar absorption coefficients for the melts and the temperatures employed. The results are presented in Fig. 4. Increasing the temperature resulted in a somewhat higher concentration of uranyl(V) ions. Under similar starting conditions (initial uranyl(VI) concentration and temperature), the concentration of U(V) ions was higher in the melt with the larger cations, the NaCl–2CsCl eutectic.

Table 2 Decomposition of uranyl(VI) chloro-species in alkali chloride melts with Zr getter positioned in the atmosphere above the melt.

Melt	T, °C	Time held under vacuum, min	U conc., wt %		Fraction of U remaining in melt, %
			initial	final	
3LiCl–2KCl	550	180	0.77	0.32	62
	750	380	0.74	0.23	23
NaCl–KCl	750	336	0.78	0.32	42
	750	410	0.81	0.34	42
NaCl–2CsCl	550	123	0.74	0.74	100
	650	218	0.79	0.77	98
	650	235	0.92	0.84	91
	750	170	0.65	0.51	78

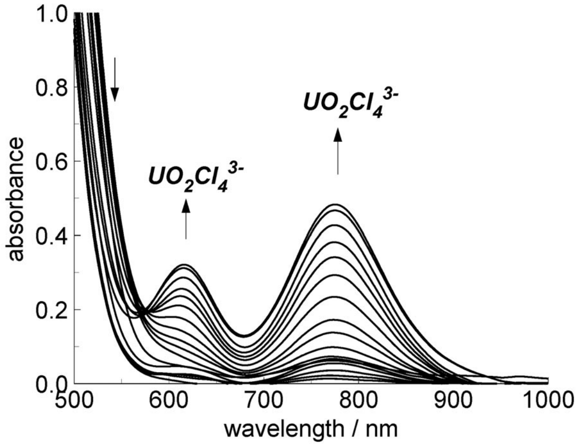

Fig. 3 Changes in the spectra of NaCl–2CsCl melt containing $UO_2Cl_4^{2-}$ with Zr getter positioned above the melt, 650 °C, total time of reaction 244 min. Arrows indicate spectral changes with time.

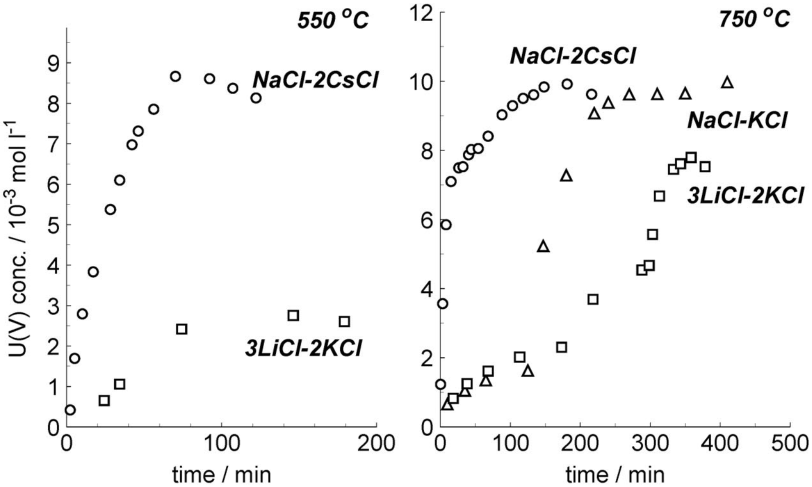

Fig. 4 Changes of U(V) concentration in chloride melts containing UO_2Cl_2 with Zr getter positioned above the melt.

These experiments thus show that the decomposition of uranyl(VI) chloro-species in alkali chloride melts proceeds according to reactions 3 and 4 and results in the formation of soluble uranyl(V) chloride and insoluble uranium dioxide.

Reaction of uranyl(VI)-containing melts with metals

The various elements present in spent nuclear fuel or used as construction materials can react with uranyl-containing melts resulting in the reduction of U(VI) ions. In the present work, a number of elements, representing various groups of fission products, were investigated. These were tellurium, palladium, silver, molybdenum, niobium, and zirconium with tellurium and palladium being the most electropositive amongst these, and niobium and zirconium the most electronegative. The reaction of metallic platinum and molybdenum with uranyl(VI)-containing melts was noted by Smirnov and Skiba [17], but the mechanism was not studied and the products formed were not characterized.

Palladium and tellurium

The standard redox potential of tellurium in alkali chloride melts is more positive than that of palladium. Elemental tellurium in molten NaCl–2CsCl containing uranyl chloride at 550 °C reacted slowly. After 3 h the oxidation state of uranium in the melt had decreased to 5.92 and the absorption spectra contained two well-pronounced bands corresponding to the uranyl(V) complex, $UO_2Cl_4^{3-}$, Fig. 5. Uranium concentration in this melt decreased from 0.86 to 0.79 wt %. Palladium reacted similarly, but the reaction rate was somewhat faster. After around 3.5 h of contact with palladium foil, the oxidation state of uranium in the uranyl(VI)-containing melt at 550 °C decreased from 6 to 5.68 and the spectra contained the absorption bands of $UO_2Cl_4^{3-}$ and $PdCl_6^{4-}$, Fig. 6. Electronic absorption spectra of palladium in fused chlorides were reported in a number of works [18] and in the visible region arise from ${}^1A_{1g} \rightarrow {}^1A_{2g}$ and ${}^1A_{1g} \rightarrow {}^1E_g$ electronic transitions in tetragonally distorted $PdCl_6^{4-}$ ion. The concen-

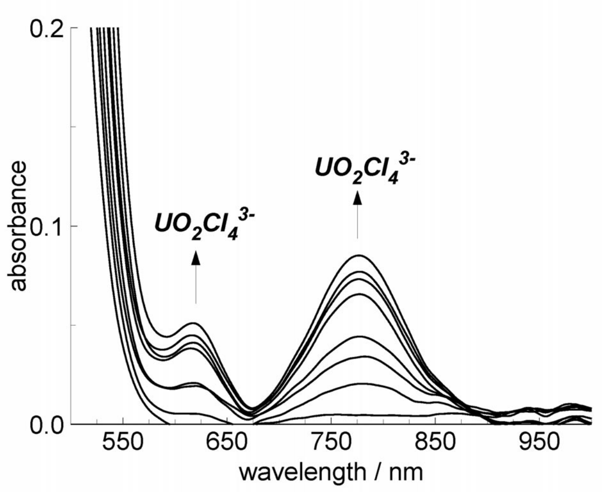

Fig. 5 Spectra showing increasing concentration of $UO_2Cl_4^{3-}$ with time, by the reaction of Te with UO_2Cl_2 in the NaCl–2CsCl melt at 550 °C. Total reaction time: 180 min.

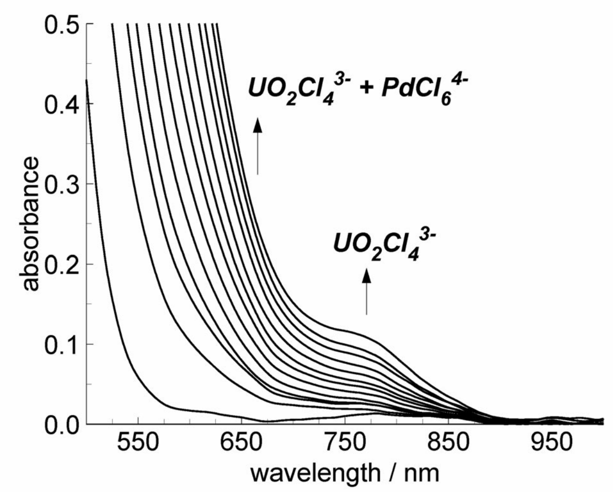

Fig. 6 Spectra showing increasing concentration of $UO_2Cl_4^{3-}$ and $PdCl_6^{4-}$ with time, for the reaction of Pd with UO_2Cl_2 in the NaCl–2CsCl melt at 550 °C. Total reaction time: 216 min.

tration of uranium remaining in the melt also decreased slightly, from 0.98 to 0.91 wt %, due to UO_2 formation and precipitation. Tellurium and palladium therefore mainly reduce $UO_2Cl_4^{2-}$ to $UO_2Cl_4^{3-}$, and to some UO_2:

$$4UO_2Cl_4^{2-} + Te + 6Cl^- \rightarrow 4UO_2Cl_4^{3-} + TeCl_6^{2-} \quad (6)$$

$$2UO_2Cl_4^{2-} + Pd + 6Cl^- \rightarrow 2UO_2Cl_4^{3-} + PdCl_6^{4-} \quad (7)$$

Silver and molybdenum

Silver is more electronegative than palladium. Immersing silver wire into the NaCl–2CsCl + UO_2Cl_2 melt at 550 and 650 °C resulted in reduction of U(VI) to U(V) ions in the melt and solid UO_2. At 650 °C, after 243 min, the oxidation state of uranium in the melt had dropped to 5.27 and the concentration of uranium in the melt from 0.95 to 0.11 wt %. Electrode potential measurements (on silver and glassy carbon electrodes) showed that over 4 h the system had not reached equilibrium.

Molybdenum is electrochemically slightly more active than silver, and the reaction of uranyl(VI)-containing melts with Mo was studied in more detail. In NaCl–2CsCl-based melts at 550, 650, and 750 °C, the absorbance in the visible region of the spectra gradually increased and bands corresponding to the absorption of $UO_2Cl_4^{3-}$ and $MoCl_6^{3-}$ arose, Fig. 7. The absorption bands of molybdenum(III) originate from a spin forbidden $^4A_{2g} \rightarrow {}^2T_{2g}$ (around 680 nm) and a spin allowed $^4A_{2g} \rightarrow {}^4T_{2g}$ (around 590 nm) transitions [19]. Another spin-allowed transition ($^4A_{2g} \rightarrow {}^4T_{1g}$) in $MoCl_6^{3-}$ gives an absorption band around 420 nm that is completely hidden in our case. The reaction in molten NaCl–KCl at 750 °C was similar. In 3LiCl–2KCl and, especially LiCl melts at 750 °C, the observed picture was rather different. Uranyl(V) concentration in the melt rapidly reached a maximum and then started to decrease.

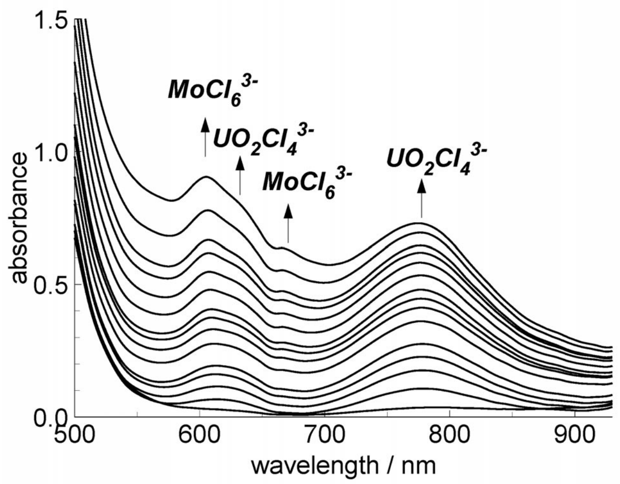

Fig. 7 Spectra recorded during the reaction of Mo metal with UO_2Cl_2 dissolved in molten NaCl–2CsCl at 650 °C. Initial U concentration 0.85 wt %. Total reduction time: 116 min.

The rate at which uranyl(V) concentration changes in the melt can be obtained from these spectra using absorbance values at around 780 nm, where uranyl(VI) and molybdenum(III) ions do not absorb. Uranium(V) concentration was determined from the spectra and the results obtained in the NaCl–2CsCl melt at varied temperatures and at 750 °C in various melts are shown in Fig. 8.

Increasing the temperature resulted in an increased rate of uranyl(V) formation in the melt, Fig. 8. Increasing the initial uranyl(VI) concentration had the same effect. Increasing the rate of U(V) formation with temperature can have two reasons, increasing the rate of the reduction process and shifting the

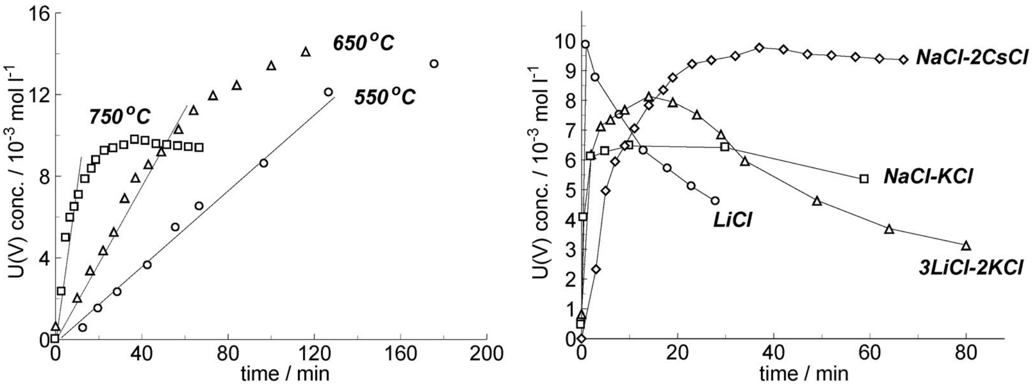

Fig. 8 The effect of temperature (left) on the extent of U(V) accumulation in molten NaCl–2CsCl and the effect of melt composition (right) on the extent of U(V) accumulation at 750 °C in various uranyl(VI)-containing melts during contact with Mo metal. Initial U concentration 0.8–0.9 wt %.

electrode potential values for the UO_2^{2+}/UO_2^{+} couple. The latter reason, however, is less probable since the difference between the redox potentials of UO_2^{2+}/UO_2^{+} and Mo^{3+}/Mo couples decreases as the temperature rises, e.g., in NaCl–2CsCl melt at 550 °C the formal standard potentials of U(VI)/U(V) and Mo(III)/Mo are equal to –0.918 and –1.015 V (vs. chlorine reference electrode), respectively, and at 750 °C they are equal to –0.825 and –0.842 V, respectively [6,20].

The uranyl(V) concentration reached a maximum and essentially stabilized in NaCl–2CsCl-based melts but then slowly decreased in NaCl–KCl melts, Fig. 8. In molten 3LiCl–2KCl, U(V) concentration decreased more rapidly than in NaCl–KCl and the time interval at which the $UO_2Cl_4^{3-}$ concentration essentially stabilized was shorter. In LiCl melt, the uranyl(V) concentration rapidly reached its maximum and then immediately started dropping. In all the systems investigated, the surface of the molybdenum wire dipped into the melt was afterwards covered with black cubic or octahedral crystals of uranium dioxide.

Electrode potentials were measured on both molybdenum and glassy carbon electrodes during these experiments. In NaCl–KCl and NaCl–2CsCl melts after 30–100 min, depending on the initial uranium concentration in the melt and the temperature, the potential values on the two electrodes became identical, indicating that the system had reached equilibrium, Fig. 9. In LiCl and 3LiCl–2KCl melts, the

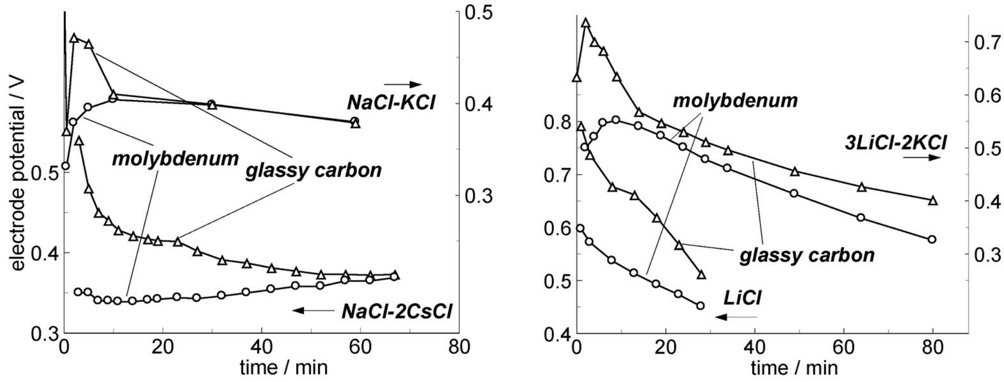

Fig. 9 Changes in electrode potentials at 750 °C in chloride melts containing UO_2Cl_2 during contact with Mo metal. Melt composition is shown for each plot.

uranium concentration in the melt constantly decreased and the difference between the potentials on molybdenum and glassy carbon electrodes was around 0.05–0.08 V, Fig. 9.

The results of experiments on reducing uranyl(VI) species in alkali chloride melts with metallic molybdenum are summarized in Table 3. Decreasing the starting U(VI) content in the melt led to an increased degree of uranium reduction, e.g., in NaCl–2CsCl melt, the average oxidation state of uranium in the final melt decreased from 5.85 to 5.04 upon lowering the initial uranium concentration from 1.71 to 0.19 wt %. At the same time, the fraction of uranium reduced to UO_2 also increased from near a quarter to almost a half. In the same melt, an increase in the temperature at a constant initial U(VI) concentration had a similar effect. Upon going from 550 to 750 °C the uranium oxidation state in the melt decreased from 5.56 to 5 and the percentage of uranium remaining in the melt from 65 to 21 %.

Table 3 Reaction of uranyl(VI)-containing melts with metallic Mo.

Melt composition	*T*, °C	U(VI) initial conc., wt.%	Time, min	U final conc., wt %	Fraction of U remaining in melt, %	Final U oxidation state	Final Mo conc., wt %
NaCl–2CsCl	550	1.71	210	1.32	77	5.85	0.024
	550	0.85	176	0.55	65	5.56	0.029
	550	0.52	267	0.32	62	5.44	0.016
	550	0.19	204	0.10	52	5.04	0.012
	650	0.85	116	0.39	46	5.05	0.051
	750	0.81	67	0.17	21	5.0	0.071
LiCl	750	0.78	28	0.10	13	n.d.	0.036
3LiCl–2KCl	750	0.92	80	0.06	7	n.d.	0.027
NaCl–KCl	750	0.93	59	0.32	34	5.1	0.020

n.d.: not determined

Measurements of the electrode potentials in NaCl–2CsCl and NaCl–KCl melts showed that by the end of the experiments the system had reached equilibrium. On the other hand, the data in Table 2 indicate that the average oxidation state of uranium in the melt was below 6 and in some experiments the final melts contained essentially only uranyl(V) species. This means that in the melt at equilibrium with uranium dioxide some uranyl(V) ions are present. As the total uranium concentration in the melt decreases, the ratio of uranyl(V)-to-uranyl(VI) concentrations in the melt increases, and at the low uranium content the melt equilibrated with uranium dioxide would contain essentially only uranyl(V) ions.

Zirconium and niobium

Apart from being the most electronegative metals tested in the present study, niobium and zirconium have a very high affinity for oxygen. We had previously demonstrated that uranyl(VI) species are unstable in chloride melts in the presence of beryllium(II) ions, with uranium(IV) chloride, beryllium oxide, and chlorine being formed [21].

Upon addition of a piece of metallic niobium into the NaCl–2CsCl + UO_2Cl_2 melt at 550 °C the absorbance in the visible region quickly increased. The spectra contained the two pronounced absorption bands of the uranyl(V) complex $UO_2Cl_4^{3-}$ overlaying a broad absorption spectrum at 500–750 nm, Fig. 10. The latter absorption is attributed to a niobium(III) and (IV) chloro-species that exist in chloride melts as octahedrally coordinated complexes $NbCl_6^{3-}$ and $NbCl_6^{2-}$, respectively [22]. The absorption bands of niobium chloro-species in the visible region in chloride melts originate from the spin allowed $^2T_{2g} \rightarrow {}^2E_g$, for Nb(IV), and $^3T_{1g} \rightarrow {}^3T_{2g}$ and $^3T_{1g} \rightarrow {}^3T_{1g}(P)$, for Nb(III), transitions. After 30 min, the absorption in the visible region began to decrease and after 2 h the spectrum included the absorption bands of the uranium(IV) chloride complex, UCl_6^{2-}, and uranyl(V) ions, $UO_2Cl_4^{3-}$. The melt color was green (characteristic of U(IV)), and a black precipitate had formed. Its analysis showed this precipitate contained uranium and niobium, probably a mixture of uranium and niobium oxides. A

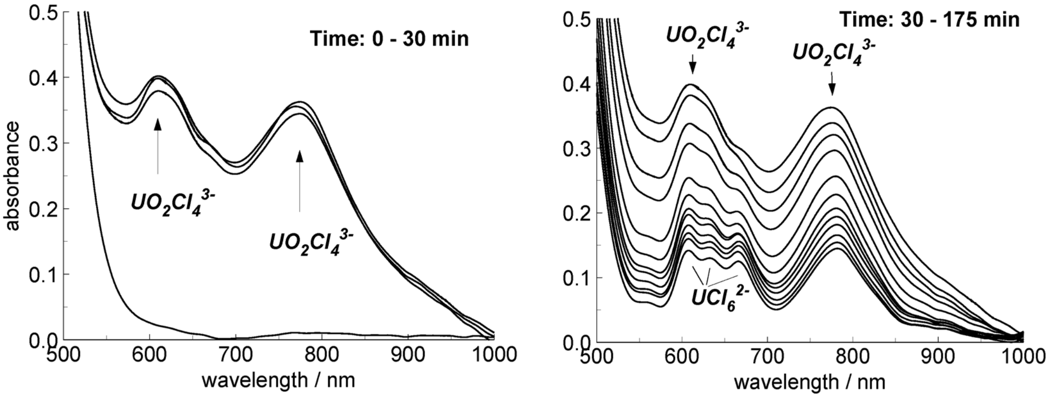

Fig. 10 Spectra recorded after contacting metallic niobium with a NaCl–2CsCl melt containing added UO_2Cl_2 at 550 °C. Upward and downward arrows show, respectively, which species are increasing or decreasing in concentration with time.

small amount of the solid phase formed did not allow structural analysis to be performed. From common niobium oxides, formation of NbO_2 and Nb_2O_5 is thermodynamically possible (for NbO, the ΔG of the reaction is far too positive). Niobium(V) oxide is white, and microscopic examination of the solid particles did not reveal any white or gray inclusions. At the present stage it was assumed that the precipitate consisted of uranium and niobium dioxides (both black). After 175 min, the oxidation state of uranium had dropped to 5.16 and the melt now contained $UO_2Cl_4^{2-}$, $UO_2Cl_4^{3-}$, UCl_6^{2-}, solid UO_2, and NbO_2. The niobium concentration in the final melt was 0.002 wt %, so essentially all the niobium was converted to NbO_2 and the absorption of the final melt was due only to $UO_2Cl_4^{2-}$, $UO_2Cl_4^{3-}$, and UCl_6^{2-} species. Increasing the temperature to 750 °C for the NaCl–2CsCl-based melt resulted in an increased reaction rate. The results are given in Table 4.

Table 4 Reaction of uranyl(VI)-containing melts with metallic Nb.

Melt composition	*T*, °C	U(VI) initial conc., wt.%	Time, min	U final conc., wt.%	Fraction of U remained in the melt, %	Final U oxidation state	Final Nb conc., wt.%
NaCl–2CsCl	550	0.96	175	0.41	43	5.16	0.003
	750	0.82	65	0.33	40	5.55	0.005
3LiCl–2KCl	750	0.87	147	0.13	45	3.63	0.004
NaCl–KCl	750	0.76	167	0.31	41	3.13	0.006

Addition of metallic niobium into a uranyl(VI) containing melt can result in a number of chemical reactions:

$$4UO_2Cl_4^{2-} + Nb + 6Cl^- \rightarrow 4UO_2Cl_4^{3-} + NbCl_6^{2-} \quad (8)$$

$$4UO_2Cl_4^{3-} + Nb \rightarrow UCl_6^{2-} + NbO_2 + 3UO_2 + 10Cl^- \quad (9)$$

$$UO_2Cl_4^{2-} + NbCl_6^{2-} \rightarrow UCl_6^{2-} + NbO_2 + 2Cl^- + Cl_2 \quad (10)$$

$$4UCl_6^{2-} + Nb + 6Cl^- \rightarrow 4UCl_6^{3-} + NbCl_6^{2-} \quad (11)$$

$$UO_2Cl_4^{2-} + 2UCl_6^{3-} \rightarrow 2UCl_6^{2-} + UO_2 + 4Cl^- \quad (12)$$

$$NbCl_6^{2-} + UO_2 \rightarrow NbO_2 + UCl_6^{2-} \quad (13)$$

In experiments performed in NaCl–2CsCl eutectic the average oxidation state of uranium in the final melt was above 5. No uranium(III) ions were observed. It is argued that the niobium metal surface was passivated by an oxide layer, preventing reaction (reaction 11).

Reaction of niobium with uranyl(VI)-containing melts based on NaCl–KCl and 3LiCl–2KCl mixtures at 750 °C also initially led to the formation of $UO_2Cl_4^{3-}$ and UCl_6^{2-} ions. However, after 3 h the melt color became red and the oxidation state of uranium was below 4, thus indicating that reaction 11 was here partially taking place.

To check the reducing ability of niobium ions toward uranyl(VI) species, a series of experiments was performed in which a sample of a UO_2Cl_2-containing melt was added to a NaCl–2CsCl melt containing the products of anodic dissolution of metallic niobium (a mixture of $NbCl_6^{3-}$ and $NbCl_6^{2-}$ according to the spectra). The initial concentration of niobium was 0.06–0.11 wt % and that of uranium 0.5–0.8 wt %. The reaction at 550 °C was very fast, and in less than 10 min the absorption bands of the uranium(IV) chloro-complex, UCl_6^{2-}, were clearly seen in the spectra. After 10–70 min, some UO_2 and NbO_2 were precipitated and the melt contained uranium(IV, V, and VI) ions. The uranium content of the melt decreased by 17–24 %, and the final niobium concentration did not exceed 0.015 wt %.

Another series of experiments was performed to check the possible occurrence of the following reaction in NaCl–2CsCl melt at 550 °C:

$$NbCl_6^- + UO_2Cl_4^{2-} \rightarrow NbO_2 + UCl_6^{2-} + {}^3/_2Cl_2 + Cl^- \qquad (14)$$

A sample of quenched NaCl–2CsCl + UO_2Cl_2 melt was added to a melt containing $NbCl_5$. No changes in the spectra were observed even after 3.5 h, and the oxidation state of uranium in the final melt was just below six (due to some thermal decomposition of uranyl(VI) chloride). Thus, we can conclude that under the conditions studied uranium(VI) and niobium(V) chloro-species can coexist in a chloride melt.

Zirconium is electrochemically more electronegative than niobium. Addition of metallic zirconium directly into the NaCl–2CsCl eutectic melt containing uranyl(VI), at 550 and 750 °C, produced a similar effect to that of niobium addition. Initially, the absorbance in the visible region increased and the spectra contained bands due to $UO_2Cl_4^{3-}$ ions formed. Then (after 60 min at 550 °C and after 11 min at 750 °C) the absorbance started to decrease and peaks associated with UCl_6^{2-} appeared. After around 3 h of contacting zirconium with the melt, the average oxidation state of uranium decreased to 5.5, Table 5, and the final green melt contained $UO_2Cl_6^{2-}$, $UO_2Cl_6^{3-}$, and UCl_6^{2-} ions and solid UO_2 and ZrO_2 (octahedral coordination of zirconium(IV) in chloride melts has been previously shown by EXAFS spectroscopy measurements [23]):

$$4UO_2Cl_4^{2-} + Zr + 6Cl^- \rightarrow 4UO_2Cl_4^{3-} + ZrCl_6^{2-} \qquad (15)$$

$$4UO_2Cl_4^{3-} + Zr \rightarrow UCl_6^{2-} + ZrO_2 + 3UO_2 + 10\ Cl^- \qquad (16)$$

The fraction of uranium remaining in the melt decreased with increasing temperature.

Table 5 Reaction of uranyl(VI)-containing melts with metallic Zr.

Melt composition	*T*, °C	U(VI) initial conc., wt.%	Time, min	U final conc., wt.%	Fraction of U remained in the melt, %	Final U oxidation state	Final Nb conc., wt.%
NaCl–2CsCl	550	0.93	185	0.57	61	5.51	n.d.
	750	0.84	180	0.18	21	5.50	0.002
3LiCl–2KCl	750	0.77	146	0.07	9	n.d.	0.004
NaCl–KCl	750	0.72	180	0.04	6	n.d.	n.d.

n.d.: not determined

Similar experiments were performed in NaCl–KCl and 3LiCl–2KCl melts at 750 °C, Table 5. After 3 h of contacting zirconium with the melt, less than 10 % of uranium remained in soluble form. Absorption spectra on using the NaCl–KCl melt contained very weak bands of UCl_6^{2-}, and the spectra of using the 3LiCl–2KCl-based melt contained none. Thus, the amount of UCl_6^{2-} ions formed in the melt can be associated with a decrease in the average cationic radius of the melt. The fraction of uranium remaining in the melt also decreased from ca. 21 % in NaCl–2CsCl to ca. 6 % in the 3LiCl–2KCl melt.

Again, although metallic zirconium should reduce U(IV) to U(III), no such reaction was observed, perhaps due to an oxide layer formed on the Zr surface.

The compatibility of $ZrCl_6^{2-}$ with $UO_2Cl_4^{2-}$ was studied in NaCl–2CsCl at 550 °C and NaCl–KCl at 750 and 850 °C. No reaction between these species was observed at initial concentrations of uranium(VI) around 0.8–1.1 wt % and zirconium up to 10 wt %. After 2–3 h, essentially all uranium (over 93 %) remained in the melt and the average oxidation state of uranium in the final melts was 5.90–5.96.

Hydrogen reduction of uranyl(VI) containing melts

The reaction of hydrogen with uranyl(VI)-containing alkali chloride melts leads to the ultimate precipitation of uranium in the form of UO_2, and this was patented as a possible mean of reprocessing spent oxide fuels [24]. The mechanism of the reaction was not, however, studied. Here we applied high-temperature spectroscopy to follow the reaction in 3LiCl–2KCl (at 550 °C), NaCl–KCl (at 750 °C), and NaCl–2CsCl melts (at 550 and 750 °C). The behavior observed in all the systems investigated was similar. After hydrogen was bubbled through the melt, U(V) species were formed and their concentration initially increased, Fig. 11. Concentration of uranyl(V) reached maximum after several minutes (4 to 15, depending on the melt and temperature) and then began to decrease, Fig 11. At the same time, precipitation of uranium dioxide commenced. From 50 to 90 min (depending on the reaction conditions) were required for complete removal of uranium from the melt. The results of the experiments are summarized in Table 6, and Fig. 12 shows how the relative concentration of U(V) in various melts changed over time.

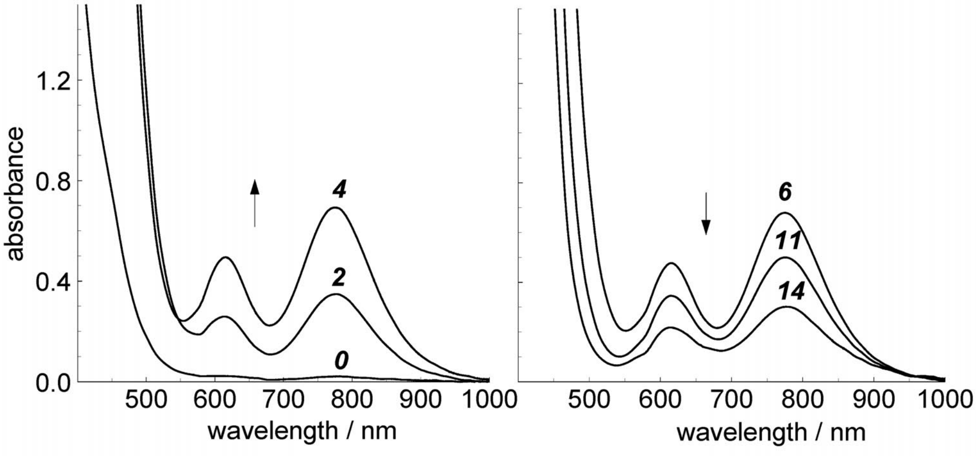

Fig. 11 Spectra recorded during reaction of hydrogen with the NaCl–2CsCl melt containing uranyl(VI) chloride at 750 °C. Arrows show direction the peaks changed with time. Total time (in min) of bubbling hydrogen through the melt is shown on each spectrum. Initial uranium concentration 0.74 wt %.

Table 6 Reaction of uranyl(VI)-containing melts with H_2.

Melt composition	*T*, °C	U(VI) initial conc., wt.%	Time, min	U final conc., wt.%	Fraction of U remained in the melt, %	Final U oxidation state	Time of reaching max. U(V) conc., min
NaCl–2CsCl	550	0.76	23	0.62	82	5.41	15
	550	0.83	45	0	0	–	9
	750	0.74	48	0	0	–	4
	750	0.71	86	0	0	–	5
3LiCl–2KCl	550	0.71	44	0	0	–	11
NaCl–KCl	750	0.42	56	0.014	3	5.62	7

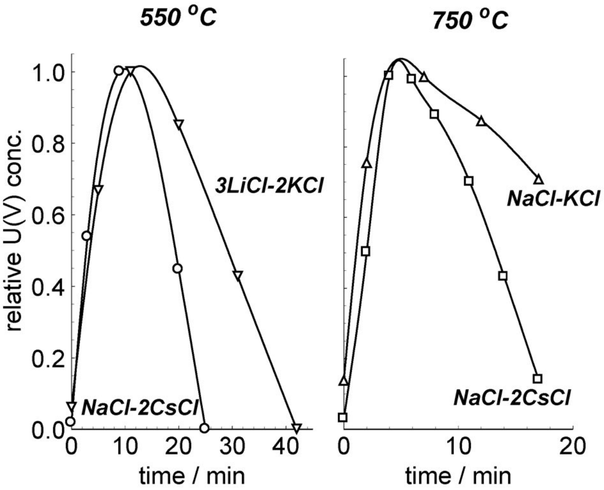

Fig. 12 Changes in relative U(V) concentration during reduction of $UO_2Cl_4^{2-}$ by H_2 over time. Temperatures and melt compositions are given for each set of data.

Reaction of uranyl(VI) chloride with hydrogen in chloride melts therefore proceeds in two stages:

$$UO_2Cl_4^{2-} + ½H_2 + Cl^- \rightarrow UO_2Cl_4^{3-} + HCl \tag{17}$$

$$UO_2Cl_4^{3-} + ½H_2 \rightarrow UO_2 + HCl + 3Cl^- \tag{18}$$

Thermodynamic calculations show that, for example, in molten NaCl–2CsCl at a total uranium concentration around 0.7 wt % $\Delta G_{(17)}$ will become equal to $\Delta G_{(18)}$ when the average oxidation state of uranium in the melt decreases to ca. 5.67 (at 550 °C) or to ca. 5.45 (at 750 °C), showing that around half of the uranium(VI) can be reduced to U(V) before reduction to UO_2 commences.

In one of the experiments performed in the NaCl–2CsCl melt at 750 °C, the absorption spectra recorded were different from the rest. Initially, the bubbling of hydrogen resulted in the typical absorption of $UO_2Cl_4^{3-}$; the concentration of this species initially increased and then started to decrease. After 15 min reduction the melt was dark red and the spectral profile had changed, Fig. 13. The absorption around 780 nm decreased but rose significantly at wavelengths below 680 nm, and the spectra exhibited three well-pronounced maxima between 360 and 600 nm. The concentration of this new uranium species in the melt initially increased and then began to decrease until all the uranium was removed from the melt after 44 min of hydrogen reduction. Attempts to reproduce this phenomenon were not successful. At present, it is difficult to characterize unambiguously that a new uranium species formed.

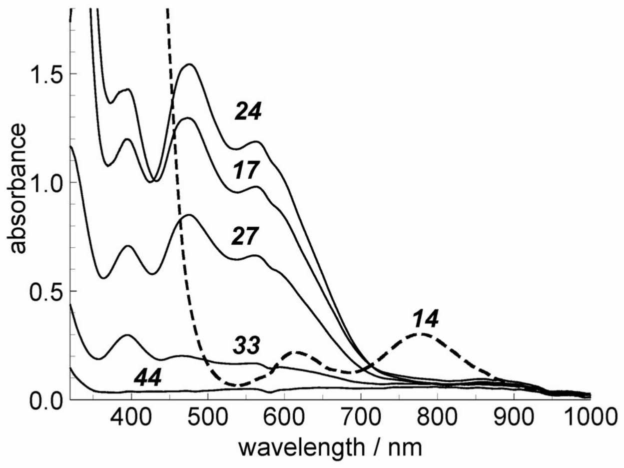

Fig. 13 Spectra recorded during reaction of hydrogen with NaCl–2CsCl melt containing uranyl chloride at 750 °C. Total time (in min) of bubbling hydrogen through the melt is given for each spectrum. Initial spectrum (14 min) is the same as in Fig. 11.

The spectra observed, however, are very similar to the absorption spectrum of $UOCl_3$ (reported in a petroleum mull [4]). It is therefore possible that the monooxouranium(V) chloro-species may be formed under certain conditions in chloride melts according to one of the following reactions:

$$3UO_2Cl_4^{3-} + H_2 \rightarrow UOCl_5^{2-} + 2UO_2 + H_2O + 7Cl^- \qquad (19)$$

$$2UO_2Cl_4^{2-} + H_2 + Cl^- \rightarrow UOCl_5^{2-} + UO_2Cl_4^{3-} + H_2O \qquad (20)$$

CONCLUSIONS

In the present work, the reactions leading to the formation of uranyl(V) chloro-species in uranyl(VI)-containing melts were studied between 550 and 850 °C. Decomposition of uranyl(VI) species by heating the starting melt under vacuum, bubbling an inert gas through the melt, or by removing Cl_2 from the atmosphere above the melt using a suitable getter resulted in partial conversion of U(VI) ions to U(V) ions and UO_2. The degree of $UO_2Cl_4^{2-}$ decomposition increased with temperature and also with decreasing the alkali cation radius of the salt solvent. No soluble U(IV) species were detected.

Contacting metallic tellurium, palladium, silver, molybdenum, niobium, and zirconium with alkali chloride melts containing uranyl(VI) chloride leads to its reduction to uranyl(V) chloride and uranium dioxide. The outcome of the reaction depends on the electrochemical properties of the reductant; the more electronegative the metal the higher the degree of U(VI) reduction. In the case of niobium and zirconium, some uranium(IV) chloride was also formed due to the high affinity of niobium and zirconium ions for oxygen.

A detailed study of the reaction of uranyl(VI)-containing melts with molybdenum showed that the degree of U(VI) conversion to UO_2 increases from NaCl–2CsCl to LiCl melt. Results obtained in NaCl–KCl and NaCl–2CsCl-based melts indicated that the melts in equilibrium with uranium dioxide contain a mixture of uranyl(VI) and (V) species or, at low uranium concentrations, essentially only uranyl(V) ions.

Bubbling hydrogen through a uranyl(VI)-containing melt resulted in a two-stage reduction U(VI) → U(V) → UO_2.

REFERENCES

1. L. R. Morss, N. M. Edelstein, J. Fuger, J. J. Katz (Eds.). *The Chemistry of Aactinide and Transactinide Elements*, 3rd ed., Vol. 1, Springer, Dordrecht (2008).
2. (a) D. Cohen. *J. Inorg. Nucl. Chem.* **32**, 3525 (1970); (b) D. Ferri, I. Grenthe, F. Salvotore. *Inorg. Chem.* **22**, 3162 (1983); (c) T. I. Docrat, J. F. W. Mosselmans, J. M. Charnock, M. W. Whiteley, D. Collison, F. R. Livens, C. Jones, M. J. Edmiston. *Inorg. Chem.* **38**, 1879 (1999); (d) A. Ikeda, C. Hennig, S. Tsushima, K. Takao, Y. Ikeda, A. C. Scheinost, G. Bernhard. *Inorg. Chem.* **46**, 4212 (2007).
3. (a) D. C. Bradley, B. N. Chakravarti, A. K. Chatterjee. *J. Inorg. Nucl. Chem.* **3**, 367 (1957); (b) J. L. Ryan. *J. Inorg. Nucl. Chem.* **33**, 153 (1971); (c) P. L. Arnold, J. B. Love, P D. Patel. *Coord. Chem. Rev*. **253**, 1973 (2009).
4. D. A. Wenz, M. D. Adams, R. K. Steunenberg. *Inorg. Chem.* **3**, 989 (1964).
5. M. D. Adams. *J. Phys. Chem.* **67**, 1939 (1963).
6. V. E. Komarov, N. P. Nekrasova. *Radiokhimiya* **25**, 233 (1983) (in Russian).
7. (a) V. A. Volkovich, I. May, J. M. Charnock. *Rasplavy* No. 2, 76 (2004) (in Russian); (b) V. A. Volkovich, I. May, C. A. Sharrad, H. Kinoshita, I. B. Polovov, A. I. Bhatt, J. M. Charnock, T. R. Griffiths, R. G. Lewin. In *Recent Advances in Actinide Science*, I. May, R. Alvarez, N. D. Bryan (Eds.), pp. 485–490, Royal Society of Chemistry, London (2006).
8. D. A. Costa, W. H. Smith, H. J. Dewey. In *Molten Salts XII*, ECS Proceedings Series 99-41, P. C. Trulove, H. C. De Long, G. R. Stafford, S. Deki (Eds.), pp. 80–99, Electrochemical Society, Pennington (2000).
9. R. S. Wilks. *J. Nucl. Mater*. **7**, 157 (1962).
10. R. W. Stromatt. *J. Electrochem. Soc*. **110**, 1277 (1963).
11. M. V. Smirnov, V. E. Komarov, A. P. Koryushin. *At. Energ.* **22**, 30 (1967) (in Russian).
12. T. Nagai, T. Fujii, O. Shirai, H. Yamana. *J. Nucl. Sci. Technol.* **41**, 690 (2004).
13. V. A. Volkovich, I. B. Polovov, B. D. Vasin, T. R. Griffiths, C. A. Sharrad, I. May, J. M. Charnock. *Z. Naturforsch., A* **62**, 671 (2007).
14. B. D. Vasin, S. P. Raspopin, V. A. Ivanov. In *VI Kola Symp. Electrochem. Rare and Non-ferrous Metals*, p. 88, KSC, Apatity (1989) (in Russian).
15. B. D. Vasin, S. V. Maslov, V. A. Volkovich, I. B. Polovov, S. A. Kazakov, O. I. Rebrin. In *Proc. 7th Int. Symp. Molten Salts Chemistry and Technology*, 29 Aug.–2 Sept. 2005, Toulouse, France, Vol. 1, P. Taxil, C. Bessada, M. Cassir, M. Gaune-Escard (Eds.), pp. 335–340 (2005).
16. A. A. Khokhryakov. *Radokhimiya* **40**, 400 (1998) (in Russian).
17. M. V. Smirnov, O. V. Skiba. *Trans. Inst. Electrochem. UBAS USSR* **4**, 17 (1963) (in Russian).
18. (a) R. A. Bailey, J. A. McIntyre. *Inorg. Chem.* **5**, 1824 (1966); (b) J. R. Dickinson, K. E. Johnson. *Can. J. Chem.* **45**, 1631 (1967); (c) J. R. Dickinson, K. E. Johnson. *Can. J. Chem.* **45**, 2457 (1967); (d) D. V. Bamburov, B. D. Vasin, A. S. Kazakov, S. P. Raspopin. *Izv. Vuzov, Tsvet. Metallurgiya* No. 4, 56 (1983) (in Russian).
19. (a) J. C. Gabriel, D. Vincent, J. Bouteillon, J. C. Poignet, V. A. Volkovich, T. R. Griffiths. *Electrochim. Acta* **44**, 4619 (1999); (b) V. A. Volkovicha, T. R. Griffiths, R. C. Thied, B. Lewin. *J. Nucl. Mater.* **323**, 93 (2003).
20. B. D. Vasin, V. A. Ivanov, I. V. Shulman, S. P. Raspopin. *Izv. Vuzov, Tsvet. Metallurgiya* No. 2, 68 (1987) (in Russian).
21. V. A. Volkovich, I. May, T. R. Griffiths, J. M. Charnock, A. I. Bhatt, B. Lewin. *J. Nucl. Mater.* **344**, 100 (2005).

22. (a) S. V. Maslov, B. D. Vasin. *Rasplavy* No. 3, 66 (1993) (in Russian); (b) G. A. Voyiatzis, E. A. Pavlatou, G. N. Papatheodorou, M. Bachtler, W. Freyland. In *Molten Salt Chemistry and Technology*, Proc. Electrochem. Soc. 93-9, M.-L. Saboungi, H. Kojima, J. Duruz, D. Shores (Eds.), pp. 252–264, Electrochemical Society, Pennington (1995); (c) C. Rosenkilde, G. Voyiatzis, V. R. Jensen, M. Ystenes, T. Ostvold. *Inorg. Chem.* **34**, 4360 (1995).
23. (a) Y. Okamoto, H. Motohashi. *Z. Naturforsch., A* **57**, 277 (2002); (b) V. A. Volkovich, I. May, T. R. Griffiths, J. M. Charnock, B. G. Lewin. In *Molten Salts XIV*, ESC Proceedings Series PV 2004-24, R. A. Mantz, P. C. Trulove, H. C. De Long, G. R. Stafford, M. Hagiwara, D. A. Costa (Eds.), pp. 162–169, Electrochemical Society, Pennington (2006).
24. A. Avogadro, V. V. Dandolo, S. Krawczynski. UK Patent 1084340, Filed 10 December 1964, Issued 20 September 1967.